Identification of F-actin as the dynamic hub in a microbial-induced GTPase polarity circuit

Robert C. Orchard, Mark Kittisopikul[#], Steve J. Altschuler[#], Lani F. Wu[#], Gurol M. Suel[#], Neal M. Alto*

Department of Microbiology and the [#]Department of Pharmacology, Green Center for Systems Biology, University of Texas Southwestern Medical Center, Dallas, TX 75390, USA.

SUPPLEMENTARY INFORMATION CONTENTS:

Figure S1: Structural comparison between bacterial and human GEF proteins, Related to Figure 1

(A and B). Structural comparison (upper) and domain organization (lower) of the *E. coli* GEF Map (PDB: 3GCG) and the human Dbl-family GEF Vav1 (PDB: 3KY9) (Yu *et al.*, 2010). The domains are color coded as shown in the domain diagrams below. PDZ^{ligand}: PSD-95, Zo-1, DLG domain binding ligands; TRL: residues threonine, arginine, and leucine in single letter amino acid code; DH: Dbl Homology domain; PH: Pleckstrin homology domain.

Supplementary Analysis:

As shown previously (Huang *et al.*, 2009), the bacterial GEF Map display a V-shaped structural architecture composed of a catalytic loop that directly interacts with residues in the guanine-nucleotide binding pocket of Cdc42. The only additional functional sequence is the PDZ-ligand that directly interacts with the PDZ domains of Ebp50. This minimal architecture is compared to the sophisticated structural architecture of Vav1, and human Dbl-family GEF that regulates several Rho-family GTPase activities. The DH domain is the catalytic region that directly interacts with Rho proteins. This domain has no resemblance to the bacterial GEFs in terms of either sequence homology or structure. In addition, Vav1 is regulated through a complex multi-domain interaction that responds consecutively to coincident signals in human cells. This behavior is in stark comparison to bacterial GEFs that are not regulated through similar mechanisms.

Figure S2: Map induces polarized filopodia bundles in a variety of cell types, related to Figure 2

a. Confocal microscopy of polarized MDCK cells expressing TAP-Map (flag-tag immunoflourescence). F-Actin (red) and Map (green) are shown at the apical and basolateral surface. Confocal sections of the apical or basolateral surface are indicated. Actin filopodia are only detected at the apical surface of Map expressing cells. Scale bar represents 10 μm. Shown to the right is a 3D reconstruction of the nano-comparmentalized acin filopodia morphology induced by Map activation of Cdc42 at the apical cell surface of polarized MDCK cells.

b. A fluorescence micrograph of an actin protrusion from a Map expressing HEK293A cell. Filopodia protrusions emanate from a lamellipodia base (marked with open arrow heads). Scale bar represents 10 μm. The emergence of filopodiia from a branched network has been extensively studied (REF Svitkina *et al* JCB 2003 and Mejillano *et al* Cell 2004)

c. Fluorsecence microscopy image of a HeLa cell expressing Map. F-actin (green) protrusions are capped with the protein Vasodilator-stimulated phosphoprotein (VASP; red). VASP is a major regulator of filopodia protusions and is localized to the tips of filopodia (REF Rottner *et al* NCB 1999). Scale bar represents 10 μm.

Figure S3: Membrane tethered Map induces microspikes, a distinct actin phenotype from Map induced filopodia, related to Figure 3

(a) Fluorescent microscopy image of a HEK293A cells transiently transfected with ^{2xPalm}Map and stained with 594-phalloidin. The bottom of the cell outline in the white box shows plasma membrane localization. Shown below each image is an enlarged image (4X) of the boxed region. The orange star marks the orientation of the box and the scale bar represents 10 µm.

(B and C). Cartoon illustrations depicting the difference between filopodia (**b**) and microspikes (**c**). Filopodia are classified as protrusions emanating from a small foci (~9 µm), while microspikes are shorter protrusions that cover large membrane distances (~28 µm). Shown to the right of each diagram is a representative fluorescent microscopy image illustrating filopodia in a Map transfected cell and microspikes in a ^{2xPalm}Map transfected cell. The boxed region is a magnified view of the protrusion and the scale bar is represents 10 µm.

(D) HEK293A cells transfected with indicated Map constructs were classified as containing filopoida or microspikes (n=3). Data are presented as mean ±SEM. The E78A mutation in Map renders the GEF domain inactive. The green arrows point out the quantification for the microspikes for the constructs. This quantification indicates that Map^{ABD} recapitulates the filopodia phenotype that wild-type Map induces, but ^{2xPalm}Map elicits predominantly a microspike phenotype.

Figure S4: Eukaryotic RhoGEFs can associate with F-actin, related to Figure 4

Domain organization of eukaryotic GEFs that can interact with F-actin either directly or indirectly. Frabin, Fgd1, and PDZ-RhoGEF, have a conserved F-actin binding domain (Obaishi *et al.*, 1998, Hou *et al.*, 2003, Banerjee *et al.*, 2009). Trio DH2, Trio DH1, Kalirin, Dbl, and Dbs have spectrin repeats which are associated with binding cytoskeletal proteins (Bellanger *et al.*, 2000, Bi *et al.*, 2001, Djinovic-Carugo *et al.*, 2002). cDEP and KIAA0793 have a FERM domain which are often associated with the cytoskeleton motifs(Diakowski *et al.*, 2006). Lastly, the GEF Lbc has been reported to associate stress fibers through an unknown mechanism (Olson *et al.*, 1997). Abbreviations: DH GEF (Dbl homology domain), PH (pleckstrin homology domain), FYVE (Fab1, YOTB, Vac1, and EEA1 domain), PDZ (PSD-95, Dlg, and ZO-1/2 domain), RGS (regulator of G protein signaling domain), C1 (protein kinase C conserved region 1), ABD (actin binding domain), Sec14 (domain in phosphatidylinositol transfer protein Sec14), Spec (spectrin repeats), SH3 (src homology 3 domain), IG (immunoglobulin domain).

Figure S5: Computational Modeling of Map induced polarity, related to Figure 5

(A) Frequency histogram displaying the correlation between the number of Cdc42 signaling zones for Map (purple) and Map^{ABD} (cyan) expressing cells (in 3 independent experiments and over 400 cells) and the number of corresponding activity peaks generated computationally from 1000 individual cells (green). For more information on how the peaks were counted please see the (**Extended Experimental Procedures Section 6.7**)

(B) Graph showing the average widths of Cdc42 signaling zones determined *in vivo* and *in silico*. 55 protrusions from 23 cells were used to calculate the mean width of Cdc42 signaling zones induced by Map in vivo. 33 protrusions from 8 simulations were used to calculate the mean width of Cdc42 signaling zones induced by Map *in silico*.

(C) Kymograph analysis of a simulation in which the distribution of Cdc42-GTP (top), Map (middle), and F-actin (bottom) is monitored over time (x-axis) in the 60 μm virtual cell (Y-axis). The green asterisks mark Cdc42 signaling zones that persist through the entire 10-minute simulation; whereas the red asterisks mark Cdc42 signaling zones that disappear during this time frame. These results are consistent with the longevity and dynamics of Cdc42 signaling zones observed in Map expressing cells (**Figure 2A**).

(D) A parameter scan in which k_{on}/k_{off} (y-axis) and γ (effective feedback; x-axis) have been varied as described in the **Extended Experimental Procedures Section 13**. The mean number of foci (left) and the average Cdc42 activity peak width (right) were counted (color bars).

Figure S6: Cue dependent GTPase polarity requires an actin-based positive feedback loop, related to Figure 6

(A) Fluorescent microscopy images of F-actin (green) in transfected cells that are engaging Fn-beads (pseudo-colored red). The vector control shows a small F-actin ring surrounding the bead revealing a seeding event. Only wild-type Map and Map^{ABD} are able to sense and respond to this seeding event, due to an actin based feedback loop. The GEF alone or the GEF linked to the membrane (^{2xPalm}Map) are unable to elicit cytoskeletal dynamics around the beads. Because of the reflective nature of the Fn-bead, we found it helpful to outline the 5 μm bead diameter with a red-dashed line.

(B) Fluorescent micrographs depicting Fn-beads recruiting eGFP-Cdc42 in Map and Map-ABD expressing cells, but not in MapE78A cells.

(C) Fluorescent micrographs depicting Fn-beads recruiting eGFP-CRIB (the Cdc42 interacting domain of N-WASP) in Map and Map-ABD expressing cells, but not in MapE78A cells.

SUPPLEMENTARY MOVIES

Supplementary Movie 1: Map polarizes F-actin protrusions, related to Figure 2. Time-lapse microscopy of an HEK 293A cell co-transfected with Map and an EGFP-ABD to show F-actin dynamics. Images were acquired every 15s for a total of 30 minutes and the movie plays at a speed of 7 frames per second.

Supplementary Movie 2: Synthetic Map constructs induce dynamic and morphologically distinct F-actin phenotypes, related to Figure 3. Time-lapse microscopy of an HEK 293A cells transfected with ^{2xPalm}Map and EGFP-ABD to show F-actin dynamics (Top) or EGFP-Map^{ABD} (Bottom). Images were acquired every 15s for a total of 15 minutes and the movie plays at a speed of 7 frames per second.

Supplementary Movie 3: Map^{ABD} moves retrograde, related to Figure 4. Time-lapse microscopy of a HeLa cell transfected with mCherry-Map^{ABD}. Images were acquired every 5s and the movie plays at a speed of 7 frames per second. Scale-bar is 5 µm.

Supplementary Movie 4: Fn-Beads stimulate F-actin dynamics in Map and Map^{ABD} expressing cells, related to Figure 6.

(A) Movie S4A shows a movie of a HEK293A cell transfected with Map. F-actin dynamics are visualized by eGFP-ABD and bright field image of Fn-Beads are pseudo-colored red.

(B) Movie S4B shows a movie of a HEK293A cell transfected EGFP-Map^{ABD} to show the recruitment of Map to the sites of Fn-Bead binding (pseudo-colored red). Images were acquired every 30s and the movie plays at a speed of 10 frames per second.

SUPPLEMENTARY TABLES

Table S1: Variables and Parameters used in the Model, related to Figure 5

Extended Experimental Procedures

1. Introduction

We seek to understand how a core set of molecular interactions between Map, actin, and Cdc42 are sufficient to explain the development of localized areas of filopodia on the membrane of eukaryotic cells expressing Map. Notably, the foci of filopodia appear to form both spontaneously and in response to a cue.

2. Overview

We model the association and dissociation of Actin and Map to and from a membrane associated area as well as the spatial distribution of a membrane diffusible species, Cdc42. This model is meant to focus on the synthetic Map-ABD that is transfected into the cell and that qualitatively recapitulates the phenotype of the wild-type Map expression. The naturally occurring system involves additional scaffolding proteins, Ezrin binding protein 50 (Ebp50) and Erzin, that link wild-type Map to actin. This scaffolding complex is not directly considered here. However, as the Actin Binding Domain (ABD) is from Erzin, we do incorporate some physical measurements from the natural system. This model applies to the wild-type system to the degree that the scaffolding proteins serve to couple Map with actin and is less applicable to the natural system if these scaffolding proteins serve other functions such as maintaining high local membrane concentrations.

Actin is represented in the model by discrete actin filaments. These are actin polymers which can associate and dissociate from the membrane. Association occurs spontaneously but is also enhanced by Cdc42 signaling due to increased actin polymerization.

Map is a discrete guanine nucleotide exchange factor for Cdc42 in the model. It activates Cdc42 by exchanging GDP for GTP. Map is positioned close to the membrane by binding to actin filaments through an actin binding domain (ABD) from Ezrin. Map is removed from the membrane through two mechanisms. One is simply unbinding from an actin filament. Unbinding represents any event by which Map is no longer able to function as a GEF for Cdc42. This may include the removal of Map to the cytosol. Another is detachment of an actin filament from the membrane to which Map molecules are bound. When an actin filament detaches, a proportional amount of Map is removed in the relevant compartment.

Activated Cdc42 is modeled as a continuous concentration that can diffuse along the membrane. Cdc42 is activated by Map. It is inactivated via hydrolysis by GAPs that are not explicitly simulated. Cdc42 is able to diffuse laterally within the membrane and in this way provides for lateral communication of molecular signaling along the membrane. Activated Cdc42 signals to a number of downstream effectors which leads to actin polymerization and thus encourages further actin filament association to the membrane.

For the purposes of simulation, we divide the cell into many small compartments along the inner surface of the plasma membrane and a cytosolic region that is functionally away from the membrane. Each membrane surface compartment represents a small volume along the membrane of a cell that contains a discrete number of actin molecules, a discrete number of Map molecules, and a concentration of Cdc42. Actin and Map move between the membrane surface compartments and further into the cytosolic region of the cell, but are only active along the membrane. In contrast, Cdc42 is the only species that directly moves from one membrane surface compartment to another through diffusion.

3. Assumptions

1. Map binds to actin filaments that associate with the cellular membrane.
2. Map acts as guanine nucleotide exchange factor for Cdc42.
3. Activation of Cdc42 by Map increases the likelihood of actin filament attachment by encouraging actin polymerization.
4. Polymerization of actin provides more binding partners for Map.
5. Unactivated Cdc42, bound to GDP, is assumed to be in excess such that the rate of Cdc42 activation by Map does not inversely depend on the active Cdc42 concentration.
6. Cdc42 diffuses laterally along the membrane.
7. Cdc42 signaling zones induced by ectopically expressed Map occur spontaneously.
8. Cdc42 signaling zones can be induced by seeding Map (as when injected by a Type 3 secretion system) or by seeding Actin (through contract with a Fibronectin bead).
9. The number of binding sites for Map on an actin filament is not limiting.
10. Actin associated Map molecules are removed from the membrane when an actin filament detaches from the membrane.
11. The total amount of Map and actin filaments are considered to be constant over the course of the simulation.

4. Variables

(See Table S1A) Time is simulated in discrete and constant timesteps such that events are relatively rare for each timestep. A spatial aspect along the membrane is introduced by dividing the membrane into many compartments identified by *x*. $a_x(t), m_x(t), and\ c_x(t)$ describe the amount of actin, Map, and Cdc42 functionally associated with each membrane surface compartment at position *x*, respectively. *A(t)* and *M(t)* describe the amount of actin and Map not functionally associated with the membrane.

5. Parameters

(See Table S1B)

1. k_{on} and k_{off} represent the spontaneous association and dissociation of actin filaments to the membrane, independent of Cdc42.
2. k_{bind} and k_{unbind} define the binding and unbinding rates of Map to an actin filament.
3. k_{gef} and k_{hydro} describe the activation of Cdc42 by Map and the deactivation of Cdc42 by GAPs, respectively.
4. *D* describes the diffusion of Cdc42 laterally along the membrane
5. k_{fb} represents active recruitment of actin filaments in a Cdc42 dependent fashion.

6. Physical Basis for Parameters

6.1 Dimensions of the Cell and Compartments

We estimated the 2D circumference of the cell as 60 µm. Approximating the cell as a disc gives a radius of 9.55 µm (which is within 10.5 ± 2.2 µm) (Zhao *et al.*, 2008, Milo *et al.*, 2010). This corresponds to a volume of 3648 μm^3 or 3.6 x 10^{-12} L. The depth of the volume near the membrane by which Map can signal to Cdc42 is approximated as 60 Angstroms or 6 nm as estimated from structural information (Figure 4A).

Since the membrane is divided up into 1000 compartments as justified in Section 6.8, each compartment spans 60 nm. The volume of each compartment, $V_{compartment}$, is therefore 60 nm x 60 nm x 6 nm = 2.16 nm^3. The membrane surface area is $(60\ nm)^2$ or 3600 nm^2

Since a $nm^3 = 10^{-24}$ L, each compartment thus has a volume of 2.16 x 10^{-20} L. Therefore a molar concentration in a compartment represents a density of 1 mol/L x 6.022 x 10^{23} molecules/mol x 2.16 x 10^{-20} L = 1.30 x 10^4 molecules per compartment. Thus, a 1 mM concentration in a compartment corresponds to about 13 molecules in that compartment. For the purposes of the stochastic description and simulation, we will describe actin and Map in terms of quantized units of molecules per compartment which corresponds to increments of 77 μM.

1 mM can also be converted into an area density in that 1 mM corresponds to about 13 molecules per 3600 nm^2 of membrane or 1 molecule per 277 nm^2 on average. Thus we can estimate that half of the average distance is the radius of a circle with area 277 nm^2. From πr^2 = 277 nm^2, r = 9.39 nm or a mean intermolecular distance of 18.8 nm. The distance scales with the square root of the molecular concentration.

6.2 Diffusion Constant of Cdc42

The most directly relatable physical constant to the dimensions of the cell is the diffusion constant of Cdc42. This has been measured to be 0.036 μm^2/sec in *S. cervisiae* and estimated be about ten times faster in *H. sapiens* due to prenylation: 0.36 μm^2 / sec (Wedlich-Soldner *et al.*, 2003, Marco *et al.*, 2007). This corresponds to a simulation unit of 100 compartments^2/sec. The diffusion constant is used as described in Section 12.

6.3 Association and Dissociation Rate of Actin Filaments

To calibrate the association rate of actin filaments, we use the binding kinetics of Arp2/3 to WASP. The K_D has been measured to be 0.25 μM while the k_{off} has been measured to be 0.6 sec^{-1} (Marchand *et al.*, 2001). This yields a calculated k_{on} rate of 2.4 μM^{-1} sec^{-1}. For the simulation the rate is converted in terms of molecules per compartment and a fixed local membrane concentration of 79 nM WASP. We use an effective association rate of 0.19 sec^{-1} or 1.9 x 10^{-4} sec^{-1} per compartment for 1000 compartments. The rate used dictates that 24% of the available actin filaments in the simulation will be associated to the membrane in the absence of feedback at steady-state conditions.

6.4 Binding of Map to Actin

The binding rates of Map to Actin are derived from K_D of 500 nM for the Ezrin Actin Binding Domain (ABD) and Actin. In the natural system, Map is associated with Ezrin and its ABD through scaffolding proteins. In the constructed system, Map is tethered directly to an ABD derived from Ezrin. k_{bind} is set to 1 $filament^{-1}$ sec^{-1} for each of the 1000 compartments and k_{unbind} to 6.5 sec^{-1} in a single compartment (Roy *et al.*, 1997).

6.5 Activation and Hydrolysis of Cdc42

The estimated k_{cat} of Map is 5-19 sec^{-1} and the estimated K_M is 6-14 μM (Friebel *et al.*, 2001, Huang *et al.*, 2009). We thus estimate the k_{cat} to be 10 sec^{-1} and the K_M to be 10 μM. The effective simulation constant for k_{gef} is 77 μM $molecule^{-1}$ sec^{-1} incorporating both the k_{cat} and K_M values since we do not simulate inactive Cdc42. The catalyzed hydrolysis rate has a k_{cat} of 2103.9 min^{-1} or about 35 sec^{-1} (Zhang *et al.*, 1997). Assuming 0.1 μM GAP present, this leads to a simulated rate of 3.5 sec^{-1}.

6.6 Feedback Term: Cdc42 to Actin polymerization

The feedback term, k_{fb} is a difficult term to relate as its physical basis depends on a number of species that signal between Cdc42 and the actin polymerization machinery that are not modeled here. This term was determined on an empirical basis based upon the mean number of filopodia foci observed in parameter variation studies (Figure S5). The rate is 0.012 μM^{-1} sec^{-1}.

6.7 Number of Foci and Width of Foci

The number and width of Cdc42 signaling zones that form foci of filopodia are measured in this work. The number is dependent on how many positive feedback loops can be initiated spontaneously before the available supply of Map and actin filaments is depleted. The number is thus dependent on the k_{on} and k_{fb} rates. High k_{on} rates increase the spontaneous association of actin filaments to the membrane and thus increases the number of foci. High k_{fb} rates increases the rate at which such an association recruits more actin filaments in competition with other spatially distinct sites. Thus high k_{fb} will eventually decrease the number of foci since foci that form earlier will attract more molecules. This is examined in a parameter variation study as shown in the Figure S5D and S5E and discussed below in Section 13.

Another consideration for the number of foci is the ability to spatially distinguish them, which is a function of foci width. The width of the foci is determined by how far an activated Cdc42 molecule can diffuse before hydrolysis inactivates it. Hydrolysis subjects active Cdc42 to exponential decay with a temporal half-life of $ln(2)/k_{hydro}$. Diffusion distributes active Cdc42 in space with a standard deviation of $\sqrt{2Dt}$.

In order to analyze foci, a low threshold (2 µM) is first used to determine when the Cdc42 concentration exceeds a certain value indicating the beginning and end of a focus. The number of compartments for which the concentration exceeds this value is considered the width of the focus. A higher threshold, 100 µM, is then used to further screen the maxima of potential foci for areas where Cdc42 is intensely concentrated. In summary, foci of filopodia are first distinguished by a low threshold and then only counted if their maxima exceed a high threshold.

6.8 Number of molecules of Map and actin filaments

Because the experimental results from this study demonstrated non-deterministic behavior in that discrete foci formed spontaneously, the number molecules involved should be small such that foci initiation is a rare event. In the simulation, the number of possible events per time step scales with the number compartments. This suggests that we select a discrete number of molecules less than the number of compartments such that it is not possible for all membrane compartments to be simultaneously occupied. This also means that we must select enough discrete compartments such that the number of molecules is physically reasonable. Since the total amount of Map and actin are fixed in the simulation, we chose the totals to be 40% of the number of compartments or 400 molecules within the cell for both Map and actin filaments. This corresponds to 400 molecules or filaments per 3.6 x 10^{-12} L in a cell or 182 pM on average and 1000 compartments.

7. Conservation of Map and Actin

$$M_T = M + \sum_x m_x \tag{1}$$

$$A_T = A + \sum_x a_x \tag{2}$$

$$M = M_T - \sum_x m_x \tag{3}$$

$$A = A_T - \sum_x a_x \tag{4}$$

For the purposes of the simulation, the total amount of Actin and Map available in the cell are considered to be fixed. Essentially, we assume that production and degradation of Actin and Map remain constant and that the cell is at or near steady state conditions for these two species. The total number of Actin and Map is thus the sum of the amount that is in equivalent compartments along the inner surface of the membrane and the amount of molecules not functionally associated with the membrane.

8. Partial Differential Equations

The following is a deterministic approximation of the model. Actin and Map are simulated stochastically as discrete molecules in a described in Section 9. Cdc42 is actually modeled as a continuous variable that represents the concentration of Cdc42 near the membrane.

$$\frac{\partial a_x}{\partial t} = (k_{on} + k_{fb} c_x) A - k_{off} a_x \tag{5}$$

$$\frac{\partial m_x}{\partial t} = k_{bind} M\, a_x - (k_{unbind} + k_{off}) m_x \tag{6}$$

$$\frac{\partial c_x}{\partial x} = k_{gef} m_x - k_{hydro} c_x + D\nabla^2 c \tag{7}$$

Actin is added in an intrinsic (k_{on} term) and Cdc42 dependent manner (k_{fb} term) based upon the number of actin filaments not associated with the membrane. Actin is removed by an intrinsic, linear rate dependent on the amount of actin in each membrane surface compartment (k_{off} term).

Map binds to actin in each membrane surface compartment in such a way that binding sites are not consumed significantly (k_{bind} term). Map can also unbind from actin in a manner proportional to the amount of Map on the membrane (k_{unbind} term). Molecules of Map can also leave the membrane through the loss of an actin filament

described by the k_{off} term for actin. A proportional amount of Map is thus removed from the membrane: $k_{off}\, a_x * m_x / a_x = k_{off}\, m_x$.

Cdc42 is activated by Map (k_{gef} term) and hydrolyzed at a linear rate that is assumed to be catalyzed by GAPs (k_{hydro} term). Cdc42 is also able to diffuse along the membrane and thus accounts for communication between the different membrane surface compartments.

9. Stochastic Description

Actin and Map are actually simulated as discrete molecules upon which stochastic Poisson processes act.

First we define the following expressions:

- $p_{am(t)} = \Pr[a_x(t) = a, m_{x(t)} = m]$, Probability of having *a* Actin and *m* Map at time *t*
- $W_{am(t)}$, Transition propensity to *a* Actin and *m* Map at time *t*
- $\dot{p}_{am} \equiv \frac{dp_{am}(t)}{dt}$, Time derivative of the probability

We can then express the stochastic simulation as follows:

$$W_{am} = k_{off}(a+1)p_{a+1,m} - (k_{on} + k_{fb}c_x)p_{am} + (k_{unbind} + k_{off})(m+1)p_{a,m+1} - k_{bind}\, a\, p_{am} \quad (8)$$

$$\dot{p}_{am} = W_{am} - W_{a,m-1} - W_{a-1,m} - W_{a-1,m-1} \quad (9)$$

c(x,t) is governed by Equation(7) . Equation(9) is the master equation that describes the stochastic evolution of Map and Actin.

10. Simulation

The simulation implements the above by simulating Map and Actin events as Poisson random processes and Cdc42 deterministically according the PDE, Eqn. (7), in a specific order:

1. Remove actin as per the k_{off} term.
    a. Remove Map proportionally with actin k_{off} events.
2. Remove Map due to unbinding from actin, k_{unbind} term.
3. Add Map due to binding with actin, k_{bind} term.
4. Hydrolyze Cdc42 according to exponential decay, k_{hydro} term.
5. Activate Cdc42 deterministically with respect to Map, k_{gef} term.
6. Diffuse Cdc42 along the membrane, *D* diffusion term.
7. Add actin by nucleation on the membrane, k_{on} and k_{fb} term.

Time progresses according to constant, discrete time steps chosen to minimize the number of events per iteration of the simulation.

11. Implementation

We implemented a fixed time increment simulation in MATLAB that simulates actin filaments and Map stochastically while treating Cdc42 deterministically. The stochastic events are determined by using a Poisson pseudo-random number with a mean propensity according to the corresponding rate law and time increment.

With this scheme it is possible for more actin or Map to be removed from a compartment than present. This is minimized by using small time increments. In case of such a rare situation, we explicitly cap the amount of a species that can be removed from a membrane surface compartment to the amount present. Similarly, for events where more of a species is moved to a membrane surface compartment from the cytosolic compartment we randomly cancel the excess number of moves. This error correction code is rarely used and does produce warnings when run.

The deterministic terms affecting Cdc42 are integrated per term in a fixed sequence. Hydrolysis is evaluated as an exponential decay. Cdc42 activation occurs deterministically based upon the presence of Map in a compartment. Cdc42 diffusion is calculated based on convolution with a Gaussian kernel as described below.

12. Note on Diffusion of Cdc42

Cdc42 is able to diffuse laterally between nearby membrane surface compartments. This is simulated by convolution with a Gaussian kernel. The Gaussian kernel is the Green's function of of the 1D diffusion equation (Strauss, 1992). The 1D diffusion equation is represented here:

$$\frac{\partial c_x}{\partial t} = D\nabla^2 \mathrm{c} \tag{10}$$

Where D represents the diffusion constant expressed in μm^2 / sec . The Gaussian kernel has standard deviation $\sigma = \sqrt{2Ddt}$. *dt* is the small time interval used for each iteration of the simulation. Thus, the kernel is expressed as

$$G(x, dt) = \frac{1}{\sqrt{4\pi Ddt}} \exp\left(-\frac{x^2}{4Ddt}\right) \tag{11}$$

The solution to the diffusion equation, Eqn. (10), is the convolution of the Cdc42 with this kernel:

$$c(x, t - t_0) = \int_{-\infty}^{+\infty} G(x - y, t - t_0) c(y, t_0) dy \tag{12}$$

However, we note that Eqn. (10) is not the solution to the full Cdc42 equation, Eqn. (7). Use of the convolution for diffusion in this case is thus an approximation which is only valid for small time steps.

Depending on *dt* the standard deviation, σ, may become less than the physical span of one compartment. Thus the simulation provides a facility by which Cdc42 may be monitored at higher spatial resolution than for Map or actin. For interaction with Map or actin the high spatial resolution Cdc42 distribution is converted to a distribution with the lower resolution of the original compartments.

13. Parameter Variation

13.1 Non-dimensional steady-state equation

We used a parameter variation study to examine how the parameters k_{on} and k_{fb} affected the number of foci that formed. More specifically, we nondimensionalized the parameters by considering the ratios of the k_{on} and k_{fb} parameters relative to k_{off} parameter. This is justified by dividing Eqn. (5) through by k_{off} and A_T and calculating the steady state proportion of actin on the membrane:

$$\frac{1}{k_{off}A_T}\frac{\partial a_x}{\partial t} = \left(\frac{k_{on}}{k_{off}} + \frac{k_{fb}}{k_{off}}c_x\right)\left(\frac{A}{A_T}\right) - \frac{a_x}{A_T} \tag{13}$$

$$\alpha(t) \equiv \frac{\sum_x a_{x(t)}}{A_T} \tag{14}$$

$$\frac{1}{k_{off}}\frac{d\alpha}{dt} = N\left(\frac{k_{on}}{k_{off}} + \frac{k_{fb}}{k_{off}}C\right)(1-\alpha) - \alpha \tag{15}$$

$$\frac{1}{k_{off}}\frac{d\alpha_{ss}}{dt} = N\left(\frac{k_{on}}{k_{off}} + \frac{k_{fb}}{k_{off}}\frac{k_{gef}}{k_{hydro}}\frac{\alpha_{ss}}{\frac{K}{A_T}+\alpha_{ss}}M_T\right)(1-\alpha_{ss}) - \alpha_{ss} \tag{16}$$

$$= 0 \tag{17}$$

Where N is the number of compartments, C is the Cdc42 concentration averaged over the compartments on the membrane (the steady state formula for this is derived below) and K is the effective dissociation constant for Map-actin binding:

$$C(t) \equiv \frac{1}{N}\sum_x c_{x(t)} \tag{18}$$

$$K \equiv \frac{k_{unbind} + k_{off}}{k_{bind}} \tag{19}$$

The effective feedback scaling factor, γ, is thus:

$$\gamma = \frac{k_{fb}}{k_{off}}\frac{k_{gef}}{k_{hydro}}M_T \tag{20}$$

$$\frac{1}{k_{off}}\frac{d\alpha_{ss}}{dt} = N\left(\frac{k_{on}}{k_{off}} + \gamma\frac{\alpha_{ss}}{\frac{K}{A_T} + \alpha_{ss}}\right)(1-\alpha_{ss}) - \alpha_{ss} = 0 \tag{21}$$

The actual steady state amount of actin on the membrane still depends on *K*. However, we can estimate the amount of actin on the membrane assuming total binding, $k_{bind} \gg k_{unbind} + k_{off}$ such that $K \approx 0$:

$$0 \approx N\left(\frac{k_{on}}{k_{off}} + \gamma\right)(1-\alpha_{ss}) - \alpha_{ss} \tag{22}$$

$$0 \approx N\left(\frac{k_{on}}{k_{off}} + \gamma\right) - \alpha_{ss}N\left(\frac{k_{on}}{k_{off}} + \gamma + \frac{1}{N}\right) \tag{23}$$

$$\alpha_{ss}\left(\frac{k_{on}}{k_{off}} + \gamma + \frac{1}{N}\right) \approx \left(\frac{k_{on}}{k_{off}} + \gamma\right) \tag{24}$$

$$\alpha_{ss} \approx \frac{\frac{k_{on}}{k_{off}} + \gamma}{\frac{k_{on}}{k_{off}} + \gamma + \frac{1}{N}} \tag{25}$$

The main difference between the k_{on} parameter and γ is that k_{on} applies equally to all membrane associated compartments, while γ is modulated by on the state of each compartment. k_{on} affects the initialization of polarity at a compartment. γ describes the strength at which a focus develops once initiated. The rate constants here are scaled for each compartment which is why the *1/N* term is present (e.g. k_{on} is the spontaneous binding rate for a single compartment whereas Nk_{on} is the spontaneous binding rate for the entire membrane). We directed our parameter variation efforts on understanding how k_{on} and γ affect the number of prominent foci.

13.2 Derivation of total steady state active Cdc42

Equation (16) is derived at steady state at conditions by first evaluating Map at steady state:

$$\frac{dM}{dt} = -k_{bind}M(A_T - A) + \left(k_{unbind} + k_{off}\right)(M_T - M) \tag{26}$$

$$\frac{1}{k_{unbind} + k_{off}}\frac{dM}{dt} = -\frac{k_{bind}}{k_{unbind} + k_{off}}M(A_T - A) + (M_T - M) \tag{27}$$

$$= -\frac{1}{K}M(A_T - A) + (M_T - M) \tag{28}$$

$$= M_T - \left(1 + \frac{1}{K}(A_T - A)\right)M = 0 \tag{29}$$

$$\frac{M_{ss}}{M_T} = \frac{1}{1 + \frac{A_T - A}{K}} \tag{30}$$

$$\frac{M_{ss}}{M_T} = \frac{K}{K + (A_T - A)} \tag{31}$$

$$\frac{M_{memb}}{M_T} = \frac{M_T - M_{ss}}{M_T} = \frac{A_T - A}{K + (A_T - A)} = \frac{\alpha_{ss}}{\frac{K}{A_T} + \alpha_{ss}} \tag{32}$$

Once we have the steady state amount of Map on the membrane, we then also derive the average steady state concentration of Cdc42 on the membrane:

$$\frac{dC}{dt} = k_{gef}(M_T - M) - k_{hydro}C \tag{33}$$

$$= 0 \tag{34}$$

$$C = \frac{k_{gef}}{k_{hydro}}(M_T - M_{ss}) \tag{35}$$

$$= \frac{k_{gef}}{k_{hydro}}\frac{\alpha_{ss}}{\frac{K}{A_T} + \alpha_{ss}}M_T \tag{36}$$

13.3 Parameter variation results

We varied the k_{on} / k_{off} ratio and γ, effective feedback, as explained above with Equation (16). The results of the effects on number of polarity sites, foci, and foci width are shown in Supplemental Figure 5D. γ was varied by changing the k_{fb} term. Ten simulations were run for each pair of parameters using a timestep of 10^{-4} seconds for 10^4 timesteps. This equates to a simulation time of one second. As expected, the number of actin filaments associated with the membrane increased directly with either k_{on} / k_{off} or γ. We also then counted the number of foci formed as discussed above in Section 6.7. Distinct and prominent foci formed at low levels of k_{on} and increased in number with γ. In this parameter regime, few foci are initiated but those that do form are able to become prominent.

At high levels of k_{on} relative to k_{off} prominent foci failed to form since many foci are initiated but they fail to become prominent or distinct. At very high levels of γ not shown in the parameter variation, the number of foci begin to decrease as one or two foci quickly become prominent and out-compete subsequent foci that may be initiated later.

At k_{on} = 0 no foci were initiated and thus no actin filaments associated with the membrane. At k_{on} / k_{off} x 1000 = 1 about half of the actin filaments are associated with the membrane. The factor of 1000 is multiplied since the k_{on} rate is always evaluated for 1000 compartments on the membrane, whereas k_{off} only applies to compartments which have actin associated with them.

Foci width increases with k_{on} and decreases slightly with γ. The increase in widths with k_{on} is mostly due to an increased likelihood of two foci being close together in space. The two foci are counted as one foci with greater width. The slight decrease in width with increasing γ is due to greater feedback intensity at the center of foci which are more concentrated in the middle. Foci width are mainly dependent on the diffusion constant, D, and the hydrolysis rate, k_{hydro}, as explained above in Section 6.7.

Map accumulated on the membrane in significant numbers because of high binding affinity as derived from the literature. The amount of active Cdc42 mainly increases with k_{on}. With higher k_{on} active Cdc42 is more evenly spread out over the membrane. This prevents GAPs from reaching V_{max} and thus decreases hydrolysis in total, allowing for more Cdc42 overall.

Overall, the parameter variation shows that distinct foci of filopodia form with a low to intermediate spontaneous association rate, k_{on} ,and a high effective feedback rate, γ, dependent on k_{fb} and Cdc42 dynamics relative to the spontaneous dissociation rate, k_{off}.

14. Ten Minute Simulation

The ten minute simulation shown in Supplemental Figure 5C was done by running the simulation at a timestep of 6 x 10^{-4} for 10^6 timesteps yielding a total simulation time of 600 seconds or 10 minutes. Three foci spontaneously form at the beginning of the simulation. The foci are shown to be dynamic over this timespan, but are relatively stable.

15. Distribution of Number of Foci

To determine the distribution of the number and width of foci as shown in Supp. Figure A and B, 1000 simulations were run with the parameters detailed above with a timestep of 10^{-4} seconds.

References

Banerjee, J., Fischer, C.C. and Wedegaertner, P.B. (2009). The amino acid motif L/IIxxFE defines a novel actin-binding sequence in PDZ-RhoGEF. *Biochemistry* 48, 8032-8043.

Bellanger, J.M., Astier, C., Sardet, C., Ohta, Y., Stossel, T.P. and Debant, A. (2000). The Rac1- and RhoG-specific GEF domain of Trio targets filamin to remodel cytoskeletal actin. *Nat Cell Biol* 2, 888-892.

Bi, F., Debreceni, B., Zhu, K., Salani, B., Eva, A. and Zheng, Y. (2001). Autoinhibition mechanism of proto-Dbl. *Mol Cell Biol* 21, 1463-1474.

Diakowski, W., Grzybek, M. and Sikorski, A.F. (2006). Protein 4.1, a component of the erythrocyte membrane skeleton and its related homologue proteins forming the protein 4.1/FERM superfamily. *Folia Histochem Cytobiol* 44, 231-248.

Djinovic-Carugo, K., Gautel, M., Ylanne, J. and Young, P. (2002). The spectrin repeat: a structural platform for cytoskeletal protein assemblies. *FEBS Lett* 513, 119-123.

Friebel, A., Ilchmann, H., Aepfelbacher, M., Ehrbar, K., Machleidt, W. and Hardt, W.D. (2001). SopE and SopE2 from Salmonella typhimurium activate different sets of RhoGTPases of the host cell. *J Biol Chem* 276, 34035-34040.

Hou, P., Estrada, L., Kinley, A.W., Parsons, J.T., Vojtek, A.B. and Gorski, J.L. (2003). Fgd1, the Cdc42 GEF responsible for Faciogenital Dysplasia, directly interacts with cortactin and mAbp1 to modulate cell shape. *Hum Mol Genet* 12, 1981-1993.

Huang, Z., Sutton, S.E., Wallenfang, A.J., Orchard, R.C., Wu, X., Feng, Y.*, et al.* (2009). Structural insights into host GTPase isoform selection by a family of bacterial GEF mimics. *Nat Struct Mol Biol* 16, 853-860.

Marchand, J.B., Kaiser, D.A., Pollard, T.D. and Higgs, H.N. (2001). Interaction of WASP/Scar proteins with actin and vertebrate Arp2/3 complex. *Nat Cell Biol* 3, 76-82.

Marco, E., Wedlich-Soldner, R., Li, R., Altschuler, S.J. and Wu, L.F. (2007). Endocytosis optimizes the dynamic localization of membrane proteins that regulate cortical polarity. *Cell* 129, 411-422.

Milo, R., Jorgensen, P., Moran, U., Weber, G. and Springer, M. (2010). BioNumbers--the database of key numbers in molecular and cell biology. *Nucleic Acids Res* 38, D750-753.

Obaishi, H., Nakanishi, H., Mandai, K., Satoh, K., Satoh, A., Takahashi, K.*, et al.* (1998). Frabin, a novel FGD1-related actin filament-binding protein capable of changing cell shape and activating c-Jun N-terminal kinase. *J Biol Chem* 273, 18697-18700.

Olson, M.F., Sterpetti, P., Nagata, K., Toksoz, D. and Hall, A. (1997). Distinct roles for DH and PH domains in the Lbc oncogene. *Oncogene* 15, 2827-2831.

Roy, C., Martin, M. and Mangeat, P. (1997). A dual involvement of the amino-terminal domain of ezrin in F- and G-actin binding. *J Biol Chem* 272, 20088-20095.

Strauss, W. (1992) Partial Differential Equations: An Introduction, John Wiley & Sons, Inc.

Wedlich-Soldner, R., Altschuler, S., Wu, L. and Li, R. (2003). Spontaneous cell polarization through actomyosin-based delivery of the Cdc42 GTPase. *Science* 299, 1231-1235.

Yu, B., Martins, I.R., Li, P., Amarasinghe, G.K., Umetani, J., Fernandez-Zapico, M.E.*, et al.* (2010). Structural and energetic mechanisms of cooperative autoinhibition and activation of Vav1. *Cell* 140, 246-256.

Zhang, B., Wang, Z.X. and Zheng, Y. (1997). Characterization of the interactions between the small GTPase Cdc42 and its GTPase-activating proteins and putative effectors. Comparison of kinetic properties of Cdc42 binding to the Cdc42-interactive domains. *J Biol Chem* 272, 21999-22007.

Zhao, L., Sukstanskii, A.L., Kroenke, C.D., Song, J., Piwnica-Worms, D., Ackerman, J.J. and Neil, J.J. (2008). Intracellular water specific MR of microbead-adherent cells: HeLa cell intracellular water diffusion. ***Magn Reson Med*** **59, 79-84.**

Supplemental Figure 1

Figure S1

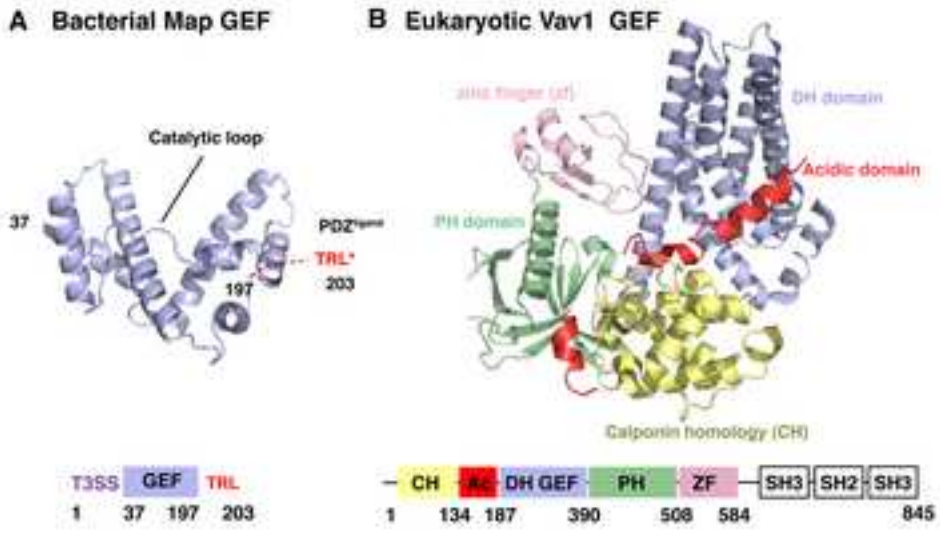

Supplemental Figure 2

Figure S2

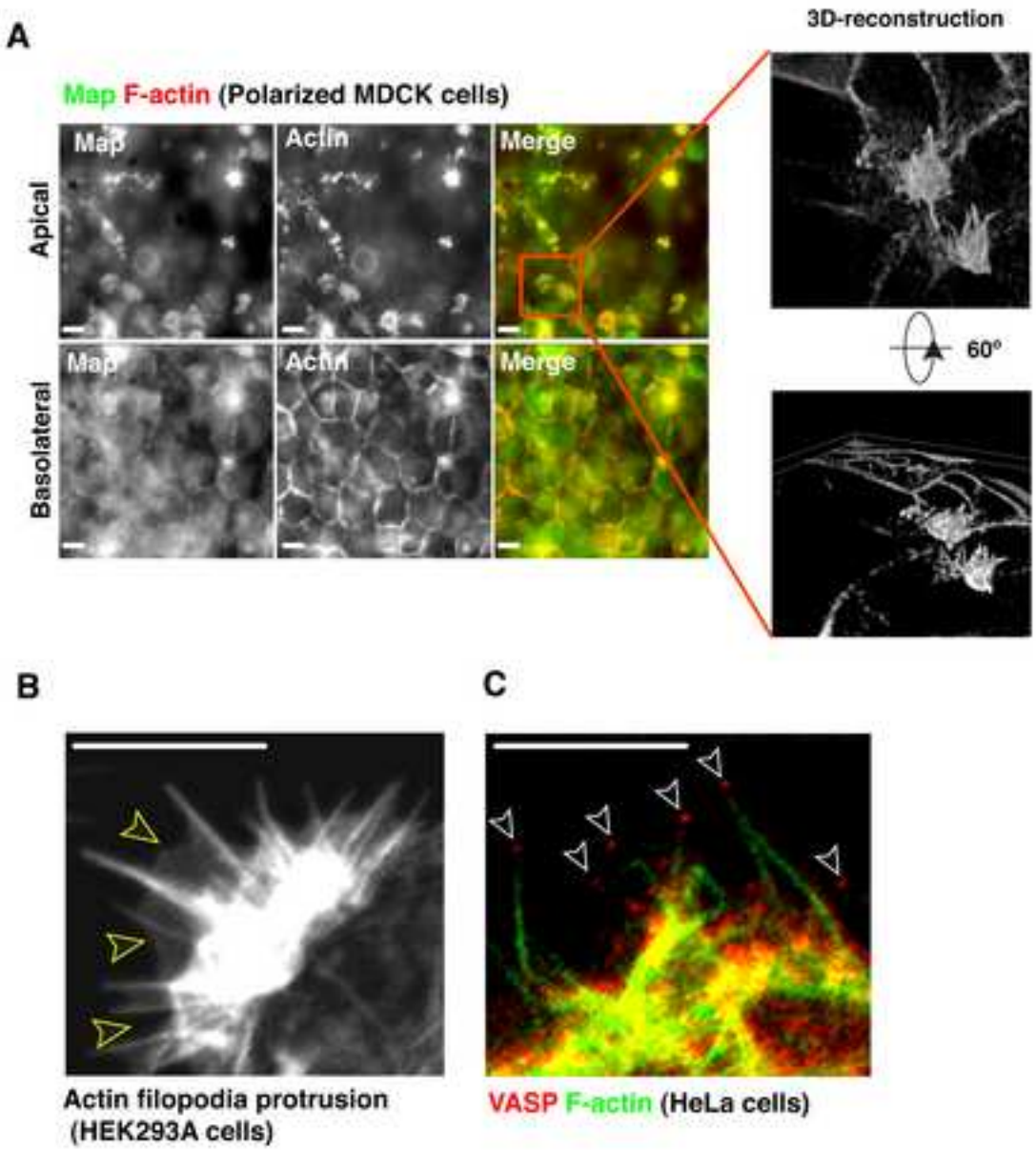

Supplemental Figure 3

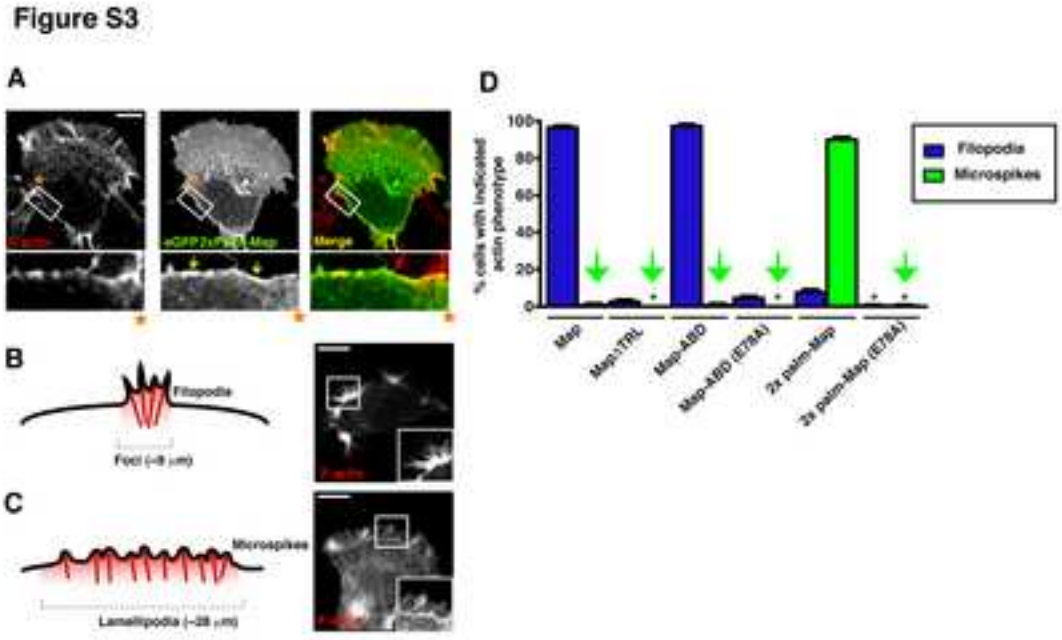

Supplemental Figure 4

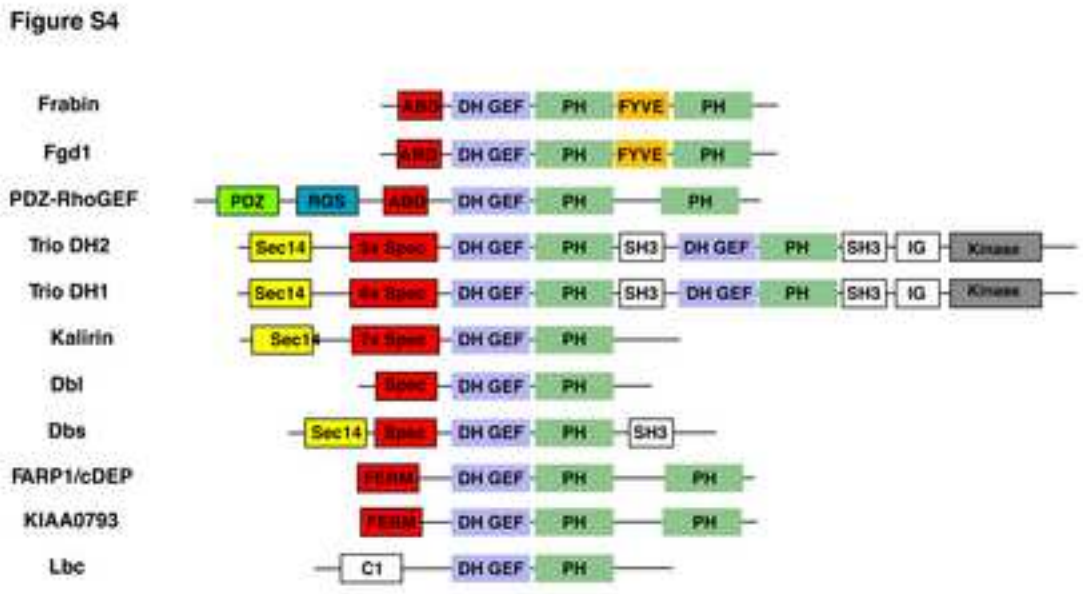

Supplemental Figure 5

Figure S5

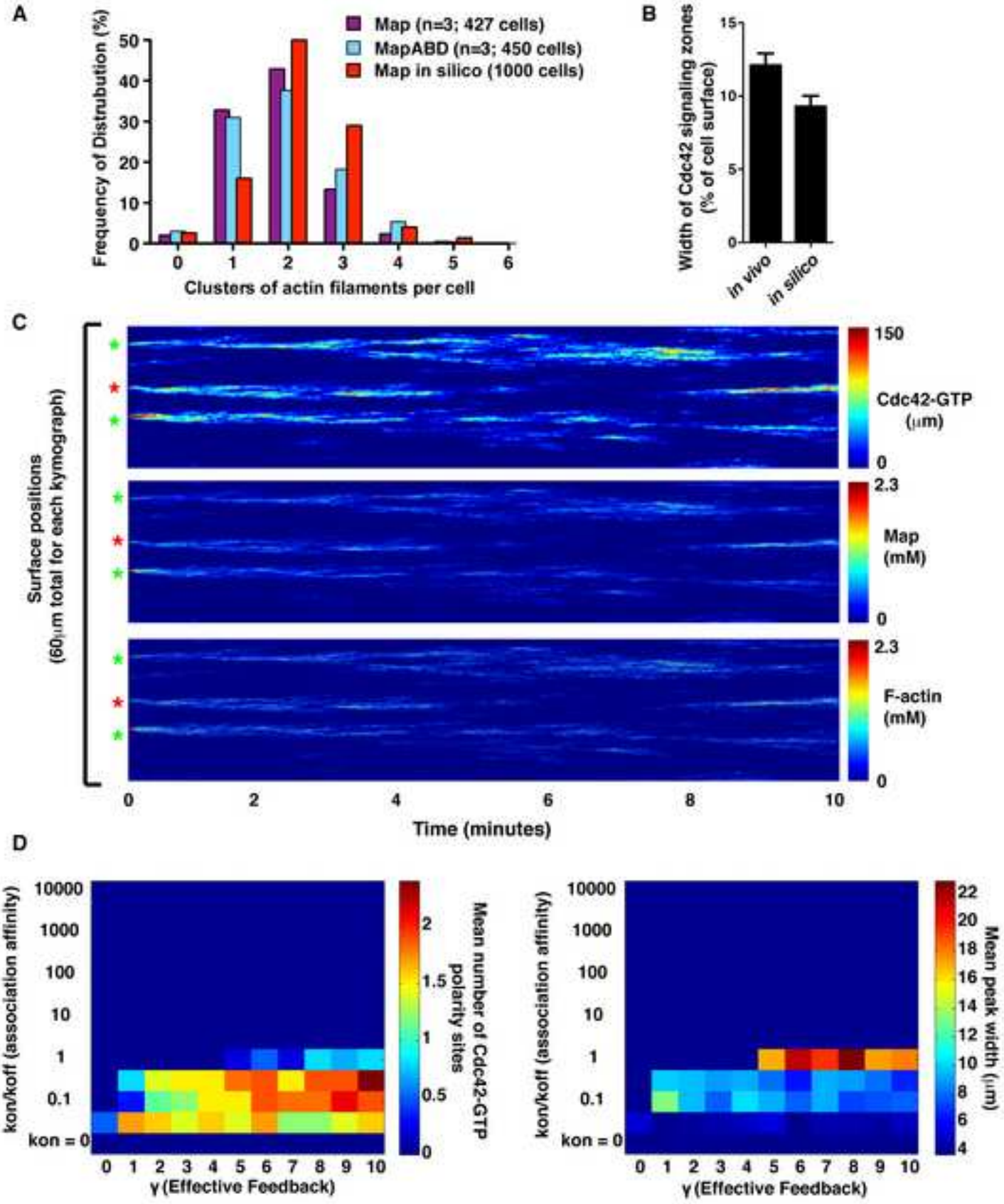

Supplemental Figure 6

Figure S6